

The Strange Sea Density and Charm Production in Deep Inelastic Charged Current Processes

M. Glück, S. Kretzer and E. Reya

Institut für Physik, Universität Dortmund
D-44221 Dortmund, Germany

Abstract

Charm production as related to the determination of the strange sea density in deep inelastic charged current processes is studied predominantly in the framework of the $\overline{\text{MS}}$ fixed flavor factorization scheme. Perturbative stability within this formalism is demonstrated. The compatibility of recent next-to-leading order strange quark distributions with the available dimuon and $F_2^{\nu N}$ data is investigated. It is shown that final conclusions concerning these distributions afford further analyses of presently available and/or forthcoming neutrino data.

Heavy quark production at high energy neutral current reactions was recently shown [1] to be optimally described within the framework of a fixed flavor (factorization) scheme (FFS) where, besides the gluon g , only the u , d and s quarks are considered as partons and any heavy quark (c , b , ...) contribution is calculated in fixed order α_s perturbation theory. Within this framework the charged current production of a heavy quark pair such as $t\bar{b}$ in $\nu p \rightarrow \mu^- t\bar{b} X$ follows the same pattern [2] utilizing the relevant formulae for the underlying 'Wg fusion' subprocess $W^+g \rightarrow t\bar{b}$. Since both $m_{t,b} \gg \Lambda_{QCD}$, we do not encounter any mass singularities here and a treatment within the framework of the FFS is straightforward and unproblematic. This favorable situation changes, however, when considering the corresponding charm production process (e.g. $W^+g \rightarrow c\bar{s}$) since the associated strange quark is taken as massless in the FFS and considered as a parton. In contrast to the former cases we encounter here a mixed situation which affords a careful treatment within the framework of the FFS. The leading order (LO) contribution for charm production in $\nu N \rightarrow \mu^- c X$, $N = (p+n)/2$, comes from the basic $\mathcal{O}(\alpha_s^0)$ subprocess $W^+s' \rightarrow c$ where

$$s'_{\nu N} \equiv |V_{cs}|^2 s + |V_{cd}|^2 \frac{d+u}{2} \quad (1)$$

with $|V_{cs}| = 0.9743$ and $|V_{cd}| = 0.221$. The $W^+g \rightarrow c\bar{s}$ fusion process yields the essential part of the next-to-leading order (NLO) correction where the other part is due to the subprocess $W^+s' \rightarrow gc$. Both subprocesses possess a mass singularity associated with $m_s = 0$ which is absorbed via dimensional regularization into the renormalized, Q^2 -dependent, parton distribution s' . The remaining finite pieces of $W^+g \rightarrow c\bar{s}$ and $W^+s' \rightarrow gc$ then yield the genuine NLO correction to $W^+s' \rightarrow c$ which will henceforth be considered in the now commonly adopted $\overline{\text{MS}}$ factorization scheme. Denoting the contributions of the above subprocesses to the structure functions $F_i(x, Q^2)$ by $F_i^c(x, Q^2)$ and defining furthermore $\mathcal{F}_1^c \equiv F_1^c$, $\mathcal{F}_3^c \equiv F_3^c/2$, $\mathcal{F}_2^c \equiv F_2^c/2\xi$ where $\xi = x(1 + m_c^2/Q^2)$, one obtains in NLO [3]

$$\begin{aligned} \mathcal{F}_i^c(x, Q^2) = & s'(\xi, \mu^2) + \frac{\alpha_s(\mu^2)}{2\pi} \left\{ \int_{\xi}^1 \frac{d\xi'}{\xi'} \left[H_i^g(\xi', \mu^2, \lambda) s'(\frac{\xi}{\xi'}, \mu^2) \right. \right. \\ & \left. \left. + H_i^g(\xi', \mu^2, \lambda) g(\frac{\xi}{\xi'}, \mu^2) \right] \right\} . \end{aligned} \quad (2)$$

Here $\lambda \equiv Q^2/(Q^2 + m_c^2)$ and the $H_i^{q,g}$ are given, up to minor modifications specified in the Appendix, in ref. [3]. The specific choice for the factorization scale μ will be studied below. The inclusive cross section in terms of the $F_i(x, Q^2)$ is given by

$$\frac{d^2\sigma^{\nu(\bar{\nu})}}{dx dy} = \frac{G_F^2 M_N E_\nu}{\pi(1 + Q^2/M_W^2)^2} \left[(1-y)F_2^{\nu(\bar{\nu})} + y^2 x F_1^{\nu(\bar{\nu})} \pm y(1 - \frac{y}{2})x F_3^{\nu(\bar{\nu})} \right] . \quad (3)$$

To study the size of the NLO corrections we shall utilize the LO and NLO parton distributions of [4] which are already conceived in the FFS being furthermore $\overline{\text{MS}}$ distributions in the NLO. In addition we shall also employ the LO and NLO($\overline{\text{MS}}$) CTEQ3 [5] and the NLO($\overline{\text{MS}}$) MRS(A) [6] parton densities which refer to the 'variable flavor' scheme where intrinsic charm densities are purely radiatively generated using the ordinary massless evolution equations, starting at $Q = m_c$. For definiteness we show in fig. 1 the quantity

$$\xi s(\xi, Q^2)_{eff} \equiv \frac{1}{2} \frac{\pi(1 + Q^2/M_W^2)^2}{G_F^2 M_N E_\nu} |V_{cs}|^{-2} \frac{d^2\sigma^{(c\bar{s})}}{dx dy} \quad (4)$$

which has been also studied experimentally [7] and where the superscript $c\bar{s}$ refers just to the CKM non-suppressed (V_{cs}) component of s' in eqs. (1–3). Note that in LO the cross section in (4) reduces to

$$\xi s(\xi, Q^2)_{eff} = \left(1 - \frac{m_c^2}{2M_N E_\nu \xi}\right) \xi s(\xi, \mu^2) + \mathcal{O}(\alpha_s) . \quad (4')$$

As can be seen in fig. 1 the NLO corrections to the LO results are reasonably small and, in particular, do not afford a drastic change of $s(x, Q^2)$ when passing from the LO to the NLO analysis.

This contrasts with the conclusions of the CCFR group [7] whose NLO $s(x, Q^2)$ is almost twice as large as compared to their previous [8] LO $s(x, Q^2)$. The analysis of the CCFR group is based on the NLO formalism of [9] which is not strictly equivalent to our NLO($\overline{\text{MS}}$) FFS formalism but still is expected to yield quite similar results. The enhancement of the NLO $s(x, Q^2)$ in [7] can therefore not be attributed to the different formalism itself [10] but rather to its inconsistent application. In the formalism of ref. [9] one considers the $W^+g \rightarrow c\bar{s}$ contribution with $m_s \neq 0$, i. e. employs a finite mass

regularization and subtracts from it that (collinear) part which is already contained in the renormalized, Q^2 -dependent $s(x, Q^2)$. The CCFR group applied their acceptance corrections to the full contribution from $W^+g \rightarrow c\bar{s}$, which corresponds effectively to a multiplication with an acceptance correction factor $\mathcal{A} = 0.6 \pm 0.1$, while inconsistently keeping the subtraction term in its full original (acceptance uncorrected) strength [11]. This latter subtraction term is given, relative to $\xi s(\xi, \mu^2)$, by

$$\text{SUB} \equiv \frac{\alpha_s(\mu^2)}{2\pi} \ln \frac{\mu^2}{m_s^2} \int_{\xi}^1 \frac{dz}{z} g(z, \mu^2) P_{qg}^{(0)}\left(\frac{\xi}{z}\right) \quad (5)$$

using [11] $m_s = 0.2$ GeV. In fig. 2 we compare the result obtained in this manner with the one where also the subtraction term [9] in (5) was consistently multiplied by the same acceptance factor \mathcal{A} . The result corresponding to the acceptance uncorrected subtraction term (dashed curve) clearly demonstrates that SUB alone [eq. (5)] represents too strong a suppression of the mass singularity component in LO + \mathcal{A} * NLO and that the correct result (solid curve) in fig. 2 is almost a factor of 2 larger in the small- x region. This implies that instead of $s_{\text{NLO}} \simeq 2 s_{\text{LO}}$ for $x \lesssim 0.1$, as inferred by CCFR [7] and used for our analysis in fig. 2, one rather needs a smaller s_{NLO} , i. e. closer in size to s_{LO} , in order to reduce the solid curve in fig. 2 and to bring it closer to experiment. Here we have chosen [7] a factorization scale $\mu = 2 p_T^{\text{max}} = \Delta(W^2, m_c^2, M_N^2)/W$, where p_T^{max} is the maximum available transverse momentum of the final state charm quark; the results in fig. 2 remain practically unaltered with the alternative choice $\mu^2 = Q^2 + m_c^2$.

A further feature emanating from the fits in [7] was $m_c^{\text{NLO}} \simeq 1.7$ GeV as compared to the previous [8] $m_c^{\text{LO}} \simeq 1.3$ GeV which further suppressed the NLO cross section and demanded the unusual, even more enhanced NLO $s(x, Q^2)$. A consistent treatment of the acceptance correction would most probably also lower the fitted m_c^{NLO} down to a more reasonable $m_c^{\text{NLO}} \simeq 1.5$ GeV and bring the NLO $s(x, Q^2)$ close to the LO $s(x, Q^2)$.

Our conclusions concerning the strange quark distributions of [4, 5] are that they agree in LO with [8] and are not refuted in NLO by the analysis in [7]. Furthermore due to the perturbative stability demonstrated in fig. 1 we expect the NLO strange quark distributions of [4–6] to lie in the correct ball park. For a final conclusion concerning these

matters, a reanalysis of presently available dimuon neutrino data is obviously mandatory!

It is also interesting to check the above statements by an independent quantitative test sensitive to $s(x, Q^2)$ such as for example the combination $\frac{5}{6}F_2^{\nu N} - 3F_2^{\mu N}$ which is given approximately by

$$\frac{5}{6} F_2^{\nu N}(x, Q^2) - 3 F_2^{\mu N}(x, Q^2) \simeq xs(x, Q^2) \quad (6)$$

where the charm contributions, the m_c^2/Q^2 corrections and the NLO q^- and g^- induced contributions are rather small and, furthermore, $|V_{cs}|^2 \simeq 1$ and $|V_{cd}|^2 \simeq 0$. In fig. 3a we compare various LO and NLO results for $xs(x, Q^2)$ in eq. (6) with the published [12] and more recent but preliminary [13] $\bar{\nu}N$ data and the NMC (deuteron) μN data [14]. It should be kept in mind that the neutrino data refer to a Fe-target and are therefore very sensitive to nuclear (EMC) corrections in the small- x region: Only the preliminary (unpublished) neutrino data [13], which are larger than the published ones [12] in the small- x region, disagree with the approximate predictions, eq. (6), in fig. 3a. That this latter approximation is indeed sufficiently accurate is demonstrated in fig. 3b where $xs(x, Q^2)$ is compared with the full NLO result for $\frac{5}{6}F_2^{\nu N} - 3F_2^{\mu N}$ which has to be calculated in the following way (note that $F_2^{\nu N}$ always refers to an average over ν and $\bar{\nu}$). In the FFS we have

$$F_2^{(\bar{\nu})N}(x, Q^2) = x \sum_{q=u,d} \left\{ (q' + \bar{q}')(x, Q^2) + \frac{\alpha_s(Q^2)}{2\pi} \left[((q' + \bar{q}') * C_2^q)(x, Q^2) + 2 (g * C_2^g)(x, Q^2) \right] \right\} + 2 \xi \mathcal{F}_2^{c(-)}(x, Q^2) \quad (7)$$

with $q' = \frac{1}{2}(1 + |V_{ud}|^2)q + \frac{1}{2}|V_{us}|^2s$, using $|V_{ud}|^2 + |V_{us}|^2 = 1$ with $|V_{ud}|^2 = 0.9743$, and where \mathcal{F}_2^c is given in eq. (2) with the replacement $s' \rightarrow \frac{1}{2}(s' + \bar{s}')$. The massless coefficient functions $C_2^{q,g}$ are standard, see e. g. ref. [4], and the convolutions are defined by

$$(q * C)(x, Q^2) = \int_x^1 \frac{dz}{z} q(z, Q^2) C\left(\frac{x}{z}\right) .$$

The well known expression for $F_2^{\mu N}$ [4] is appropriately modified for an isoscalar target, with the charm contribution $F_2^{c\bar{c}}$ calculated according to the $\gamma^*g \rightarrow c\bar{c}$ fusion process

etc. [1] as described, for example, in [4]. In the 'variable flavor' scheme [5, 6], where intrinsic charm densities $c(x, Q^2)$ are generated radiatively by the ordinary massless evolution equations, we have

$$\frac{1}{x} \left(\frac{5}{6} F_2^{\nu N} - 3 F_2^{\mu N} \right) = (s - c)(x, Q^2) + \frac{\alpha_s(Q^2)}{2\pi} [(s - c) * C_2^q](x, Q^2) \quad . \quad (8)$$

In view of the preliminary and contradicting nature of the nuclear-shadowing corrected CCFR data for $F_2^{(\nu)N}$ used in fig. 3, a decision concerning the (dis)agreement with theoretical QCD predictions must obviously be postponed. According to our results in figs. 1 and 2, implying strongly that s_{NLO} is similar in size to s_{LO} , and the ones in fig. 3 which imply that the inclusion of the finite part of $W^+g \rightarrow c\bar{s}$ and the corresponding photon induced $\gamma^*g \rightarrow c\bar{c}$ in conjunction with present NLO strange quark densities [4–6] do not change significantly the simple LO results, the theoretical predictions are rather constrained and unique. Furthermore, the results in fig. 3 again support our previous conclusions [1] concerning the perturbative stability [3, 15] of the charm production rate as calculated in perturbative fixed order α_s , i. e. in the FFS. A similar analysis was carried out in [16] where different conclusions concerning the magnitude of the gluon induced contributions are presented: These results are almost a factor of two larger than the full NLO results at $x = 10^{-2}$ in fig. 3b since a factor of two error seems (due to the lack of explicit formulae in [16] it is not possible to trace its exact origin) to be present in the calculation of the $W^+g \rightarrow c\bar{s}$ contribution. Therefore, if the enhanced preliminary νN data at $x \lesssim 0.1$ as shown in fig. 3 are confirmed, the discrepancy between these data and the rather solid and unique theoretical results, taking into account the rather well understood dimuon data as well, will constitute a major problem which cannot be solved within our present understanding of the so far successful perturbative QCD.

Acknowledgements

We thank A. O. Bazarko for several correspondences and private communications. This work has been supported in part by the 'Bundesministerium für Bildung, Wissenschaft, Forschung und Technologie', Bonn.

Appendix

The fermionic NLO coefficient functions H_i^q for heavy quark (charm) production in eq. (2), calculated from the subprocess $W^+s \rightarrow gc$, are given by

$$H_i^q(z, \mu^2, \lambda) = \left[P_{qq}^{(0)}(z) \ln \frac{Q^2 + m_c^2}{\mu^2} + h_i^q(z, \lambda) \right] \quad (\text{A1})$$

where $P_{qq}^{(0)}(z) = \frac{4}{3} \left(\frac{1+z^2}{1-z} \right)_+$ and

$$h_i^q(z, \lambda) = \frac{4}{3} \left\{ h^q + A_i \delta(1-z) + B_{1,i} \frac{1}{(1-z)_+} + B_{2,i} \frac{1}{(1-\lambda z)_+} + B_{3,i} \left[\frac{1-z}{(1-\lambda z)^2} \right]_+ \right\} \quad (\text{A2})$$

with

$$h^q = - \left(4 + \frac{1}{2\lambda} + \frac{\pi^3}{3} + \frac{1+3\lambda}{2\lambda} K_A \right) \delta(1-z) - \frac{(1+z^2) \ln z}{1-z} + (1+z^2) \left[\frac{2 \ln(1-z) - \ln(1-\lambda z)}{1-z} \right]_+ \quad (\text{A3})$$

and

$$K_A = \frac{1}{\lambda} (1-\lambda) \ln(1-\lambda) \quad . \quad (\text{A4})$$

The coefficients in (A2) for $i = 1, 2, 3$ are given in Table 1 where a misprint in [3] concerning A_2 was corrected.

Table 1. Coefficients for the expansion of h_i^q in (A2)

i	A_i	$B_{1,i}$	$B_{2,i}$	$B_{3,i}$
1	0	$1 - 4z + z^2$	$z - z^2$	$\frac{1}{2}$
2	K_A	$2 - 2z^2 - \frac{2}{z}$	$\frac{2}{z} - 1 - z$	$\frac{1}{2}$
3	0	$-1 - z^2$	$1 - z$	$\frac{1}{2}$

The gluonic NLO coefficient functions H_i^g for heavy quark (charm) production in eq. (2), as calculated from the subprocess $W^+g \rightarrow c\bar{s}$, are given by

$$H_{i=1,2,3}^g(z, \mu^2, \lambda) = \left[P_{qg}^{(0)}(z) \left(\pm L_\lambda + \ln \frac{Q^2 + m_c^2}{\mu^2} \right) + h_i^g(z, \lambda) \right] \quad (\text{A5})$$

where $P_{qg}^{(0)}(z) = \frac{1}{2} [z^2 + (1-z)^2]$, $L_\lambda = \ln \frac{1-\lambda z}{(1-\lambda)z}$ and

$$h_i^g(z, \lambda) = C_0 + C_{1,i} z(1-z) + C_{2,i} + (1-\lambda) z L_\lambda (C_{3,i} + \lambda z C_{4,i}) \quad (\text{A6})$$

with

$$C_0 = P_{qg}^{(0)}(z) [2\ln(1-z) - \ln(1-\lambda z) - \ln z] \quad . \quad (\text{A7})$$

The coefficients $C_{k,i}$ are given in Table 2 and differ from those in [3] where the older convention [17] has been adopted of counting the gluonic helicity states in $D = 4$ rather than in $D = 4 + 2\varepsilon$ dimensions. The latter convention [18] is the one chosen to define all modern NLO parton distributions.

Table 2. Coefficients for the expansion of h_i^g in (A6)

i	$C_{1,i}$	$C_{2,i}$	$C_{3,i}$	$C_{4,i}$
1	$4 - 4(1 - \lambda)$	$\frac{(1-\lambda)z}{1-\lambda z} - 1$	2	-4
2	$\frac{8-18(1-\lambda)}{+12(1-\lambda)^2}$	$\frac{1-\lambda}{1-\lambda z} - 1$	6λ	-12λ
3	$2(1 - \lambda)$	0	$-2(1 - z)$	2

Note that in the limit $\lambda \rightarrow 1$ ($m_c \rightarrow 0$) the $H_i^{q,g}$ reduce, apart from the obvious collinear logs, to the massless $\overline{\text{MS}}$ coefficient functions $C_i^{q,g}$ [4, 18].

References

- [1] M. Glück, E. Reya and M. Stratmann, Nucl. Phys. B422 (1994) 37.
- [2] M. Glück, R. M. Godbole and E. Reya, Z. Phys. C38 (1988) 441; Erratum C39 (1988) 590;
G. Schuler, Nucl. Phys. B299 (1988) 21;
U. Baur and J. J. van der Bij, Nucl. Phys. B304 (1988) 451.
- [3] T. Gottschalk, Phys. Rev. D23 (1981) 56.
- [4] M. Glück, E. Reya and A. Vogt, Z. Phys. C67 (1995) 433.
- [5] H. L. Lai et al., CTEQ collab., Phys. Rev. D51 (1995) 4763.
- [6] A. D. Martin, R. G. Roberts and W. J. Stirling, Phys. Rev. D50 (1994) 6734.
- [7] A. O. Bazarko et al., CCFR collab., Z. Phys. C65 (1995) 189.
- [8] S. A. Rabinowitz et al., CCFR collab., Phys. Rev. Lett. 70 (1993) 134.
- [9] M. A. G. Aivazis, J. C. Collins, F. I. Olness and W.-K. Tung, Phys. Rev. D50 (1994) 3102.
- [10] G. Kramer, B. Lampe and H. Spiesberger, DESY 95-201.
- [11] A. O. Bazarko, Ph. D. thesis, Columbia University, Nevis-285 (1994).
- [12] E. Oltman et al., CCFR collab., Z. Phys. C53 (1992) 51.
- [13] CCFR collab. (1993), private communication from R. G. Roberts.
- [14] M. Arneodo et al., NMC, Phys. Lett. B364 (1995) 107.
- [15] B. J. Edwards and T. D. Gottschalk, Nucl. Phys. B186 (1981) 309.
- [16] V. Barone, M. Genovese, N. N. Nikolaev, E. Predazzi and B. G. Zakharov, CERN-TH/95-125 (Z. Phys. C, to appear).

- [17] G. Altarelli, R. K. Ellis and G. Martinelli, Nucl. Phys. B157 (1979) 461.
- [18] W. A. Bardeen, A. J. Buras, D. W. Duke and T. Muta, Phys. Rev. D18 (1978) 3998;
W. Furmanski and R. Petronzio, Z. Phys. C11 (1982) 293.

Figure Captions

Fig. 1 LO and NLO predictions for $\xi_{s_{eff}}$ defined in eq. (4), using the GRV [4] and CTEQ3 [5] parton densities. The dotted curves refer to using just the NLO strange quark contribution in eq. (2) with all $\mathcal{O}(\alpha_s)$ terms neglected. Thus the differences between the dashed and dotted curves illustrate the differences between the LO and NLO strange sea densities, respectively. The values of Q^2 vary between 2.4 to 43.9 GeV² according to the experimental averages [8] for $0.015 \leq x \leq 0.35$ and $E_\nu = 192$ GeV [7] has been used.

Fig. 2 NLO results using the NLO strange sea density of CCFR [7]. The subtraction term (SUB) is defined in (5) and an acceptance correction factor $\mathcal{A} = 0.6$ has been used [11]. The analysis was performed with the original subroutines/matrix elements of CCFR [11]; if the charged current structure functions of GGR [2] are used instead, the results are similar. The shaded area refers to the CCFR 'data' [8], calculated according to (4'), where the CKM suppressed contribution in (1) has been subtracted from the measured full cross section by assuming specific up and down quark densities [7, 11]. The dashed curve corresponds to the original CCFR fit analysis [7, 11].

Fig. 3 (a): LO and NLO GRV [4] and MRS(A) [6] predictions for $xs(x, Q^2)$ which approximates $\frac{5}{6}F_2^{\nu N} - 3F_2^{\mu N}$ in eq. (6). (b): Full NLO result for $\frac{5}{6}F_2^{\nu N} - 3F_2^{\mu N}$ in the FFS (dashed dotted curve) using eq. (7), and the short-dashed curve shows the corresponding result with the $W^+g \rightarrow c\bar{s}$ contribution turned off. The factorization scale chosen is $\mu^2 = Q^2 + m_c^2$. The solid curve for xs , being the same as in (a), is shown for comparison. The full NLO MRS(A) result in the 'variable flavor' scheme is based on eq. (8). Both CCFR [12] (circles) and preliminary CCFR [13] (squares) νN (Fe-target) data are corrected for nuclear shadowing effects, whereas the NMC μN data [14] have been obtained from a deuterium target.

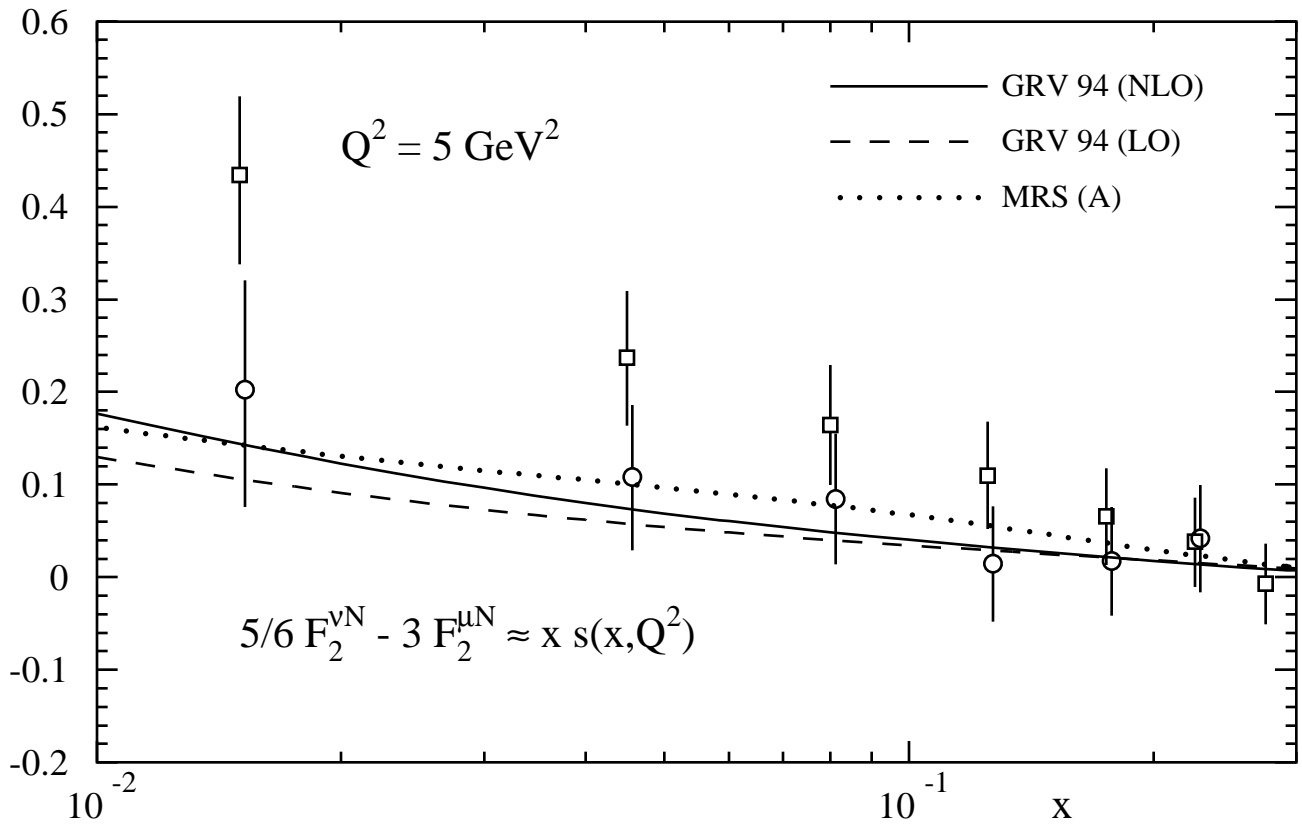


Fig. 3a

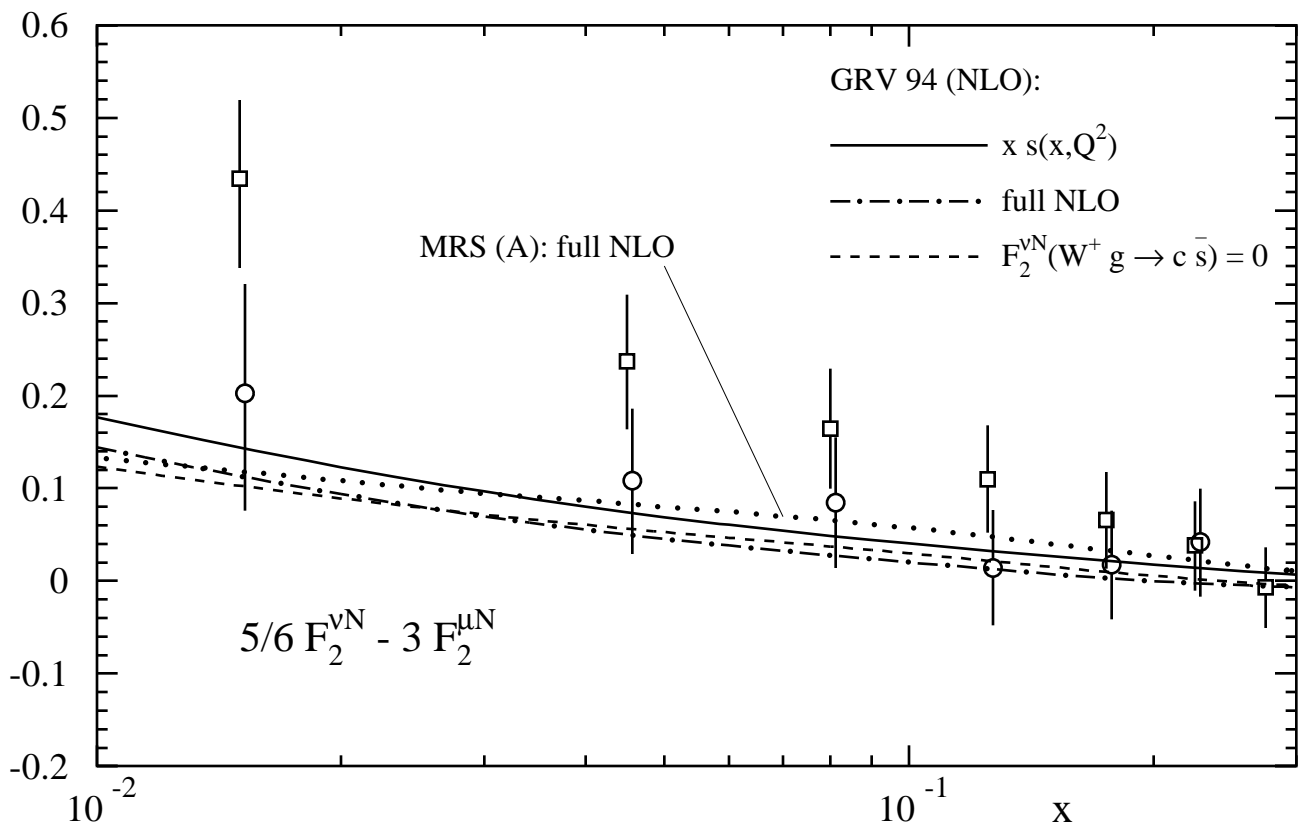


Fig. 3b

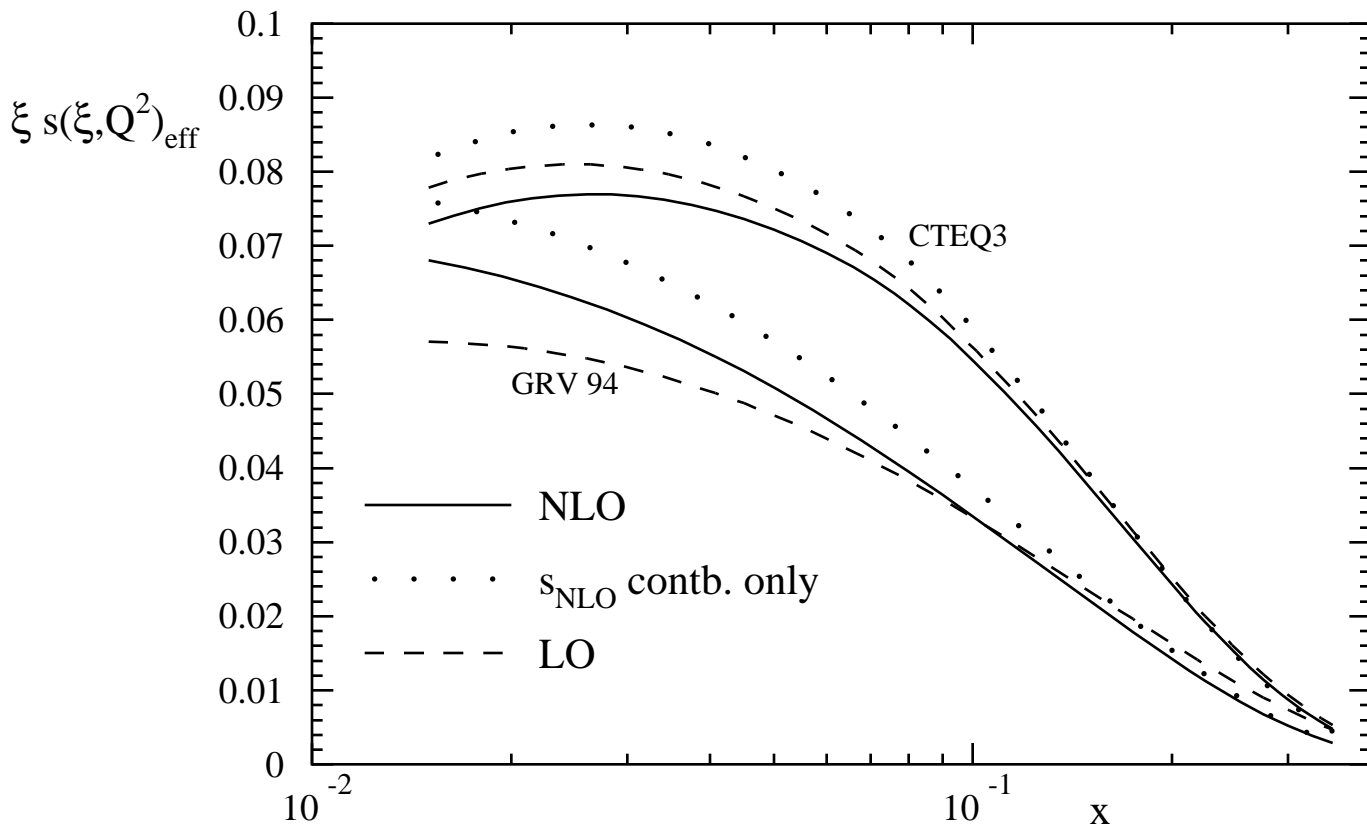


Fig. 1

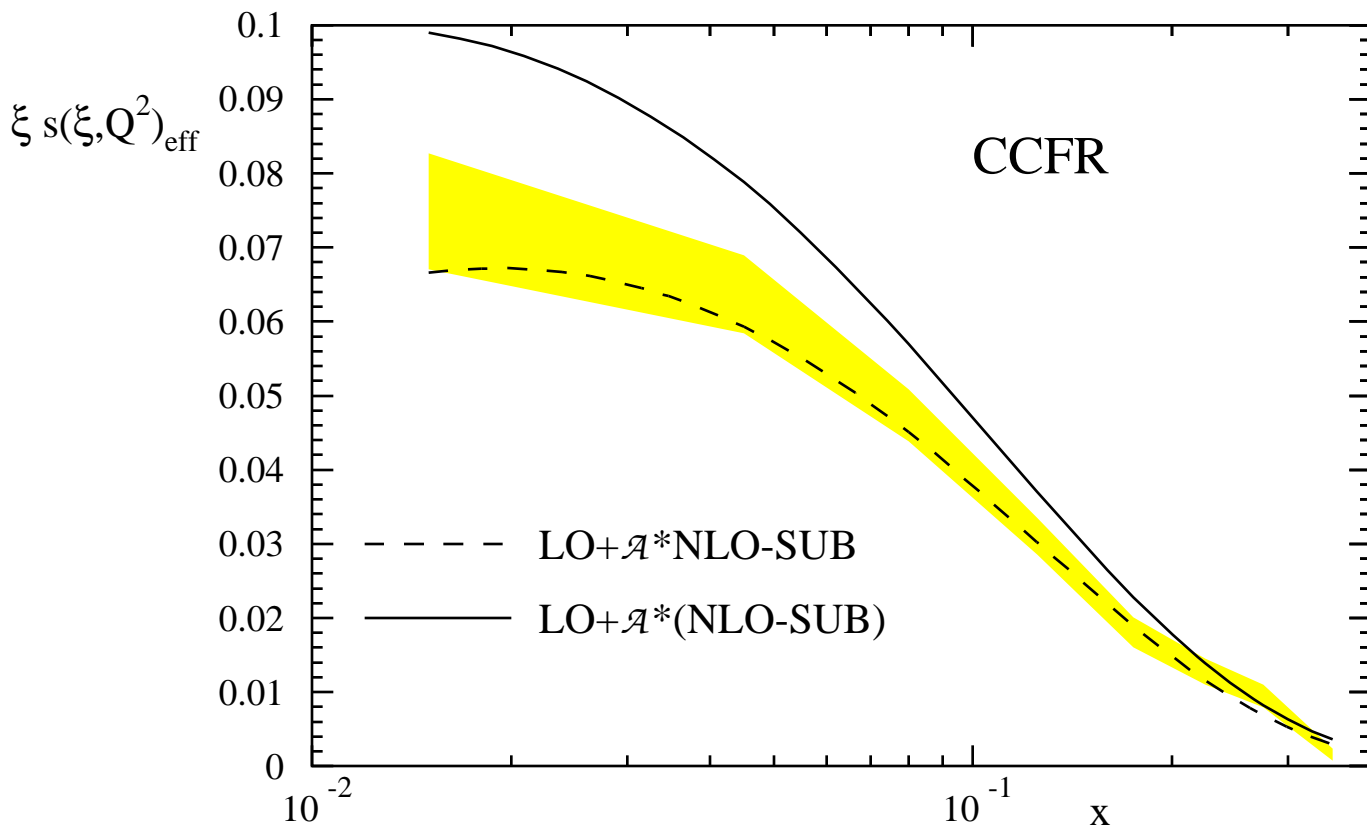


Fig. 2